

# ATBD 1995

## Thermal Calibration Algorithm

Error Analysis  
Technical Approaches  
Pre-Launch Testing

Dan Knowles, Jr.  
GSC

31JUL95

# MODIS Thermal Error Analysis Parameters

	Uncertainty	Nominal
Blackbody Temperature	.1K	295K
Cavity Temperature	10K	290K
Mirror Temperature	1K	290K
Nonlinearity	*1%	5%
Blackbody Emissivity	.004	.992
Wavelength <del>Spec.</del>	.1%	CW

Center

\* 1.5% uncertainty for the fire bands (Bands 21, 31hi, and 32hi)

Mirror relative reflectance contamination terms .1% uncertainty

Digitization error is 1.5 bits

NEdDN calculated from MODIS Specification value of NEdL

Ghosting, Crosstalk, and OOB results from 1994 SBRC MODIS CDR

Optics temperature 285K

Earth scene temperature from MODIS Specification

Optical transmissions from SBRC technical memo PL3095-Q02568

Earth scene at scan mirror nadir

Scan mirror reflectance data from Lincoln Labs

NEdL  
DNL  
LNL

# Error Analysis Results

PV Bands

Band	20	21	22	23	24	25	27	28	29	30
BB Temp	0.44	0.41	0.42	0.41	0.38	0.37	0.25	0.23	0.20	0.18
Cav Temp	0.35	0.33	0.33	0.33	0.31	0.30	0.13	0.09	0.06	0.07
Mir Temp	0.01	0.01	0.00	0.01	0.12	0.02	0.07	0.03	0.02	0.07
Nonlin	0.00	0.05	0.00	0.00	0.02	0.01	0.77	0.59	0.14	0.90
Dig/SNR	0.49	8.32	0.52	0.50	0.29	0.58	0.28	0.34	0.20	0.36
BB emiss	0.09	0.08	0.08	0.08	0.08	0.08	0.05	0.05	0.04	0.04
WL Shift	0.80	0.73	0.73	0.71	0.59	0.58	0.23	0.17	0.07	0.00
Mir ref/sv	0.02	0.06	0.02	0.01	0.51	0.10	0.38	0.21	0.01	0.14
Mir ref/ev	0.04	0.08	0.03	0.03	0.49	0.08	0.37	0.20	0.02	0.13
Ghosting	0.40	0.45	0.45	0.45	0.45	0.45	0.45	0.45	0.45	0.45
Crosstalk	0.20	0.35	0.35	0.35	0.35	0.35	0.35	0.35	0.35	0.35
OOB	0.31	0.36	0.36	0.36	0.36	0.36	0.36	0.36	0.36	0.36
Spec	0.75	10.00	1.00	1.00	1.00	1.00	1.00	1.00	1.00	1.00
RSS	1.23	8.40	1.25	1.22	1.29	1.17	1.25	1.05	0.75	1.22

% L<sub>typ</sub>

L<sub>max</sub> = 315 for L<sub>max</sub> < 315

check L<sub>bb</sub> = L<sub>typ</sub> if WL = 0

$\frac{1}{\sqrt{12}}$  + NEJDN

# Error Analysis Results

PC Bands

Band	31	32	33	34	35	36	31hi	32hi
BB Temp	0.15	0.14	0.12	0.11	0.10	0.08	0.15	0.14
Cav Temp	0.07	0.08	0.10	0.11	0.11	0.09	0.07	0.09
Mir Temp	0.01	0.01	0.04	0.06	0.08	0.14	0.00	0.00
Nonlin	0.09	0.06	0.10	0.11	0.13	0.18	9.22	3.87
Dig/SNR	0.17	0.15	0.34	0.32	0.31	0.37	3.19	2.69
BB emiss	0.03	0.03	0.02	0.02	0.01	0.02	0.04	0.03
WL Shift	0.06	0.09	0.14	0.16	0.17	0.20	0.06	0.09
Mir ref/sv	0.01	0.01	0.07	0.10	0.14	0.26	0.06	0.06
Mir ref/ev	0.01	0.01	0.05	0.07	0.09	0.16	0.07	0.06
Ghosting	0.30	0.30	0.45	0.45	0.45	0.45	0.30	0.30
Crosstalk	0.30	0.30	0.35	0.35	0.35	0.35	0.30	0.30
OOB	0.02	0.02	0.36	0.36	0.36	0.36	0.02	0.02
Spec	0.50	0.50	1.00	1.00	1.00	1.00	10.00	10.00
RSS	0.50	0.49	0.80	0.80	0.81	0.91	9.83	4.77

# Simulated Data Set for Error Analysis

Band	Gain1	Gain2	Gain3	Gain4	Vdc1	DNbb	DNSv	DNev	
20	91.3057	-7.40007559	-7.40007559	-7.400076	3.96E-05	756	100	915	
21	17.6075	-5.32887837	-5.32887837	-5.328878	3.66E-05	124	100	203	
22	14.2922	-18.7040619	-18.7040619	-18.70406	3.6E-05	993	100	1197	
23	20.5412	-15.601709	-15.601709	-15.60171	3.68E-05	1019	100	1224	
24	21.9426	-15.0952766	-15.0952766	-15.09528	4.25E-05	1640	100	323	
25	27.2269	-13.5514533	-13.5514533	-13.55145	4.3E-05	1653	100	814	
27	62.6632	-8.93261496	-8.93261496	-0.893261	0.000392	2130	100	518	
28	4.03219	-4.97999948	-4.97999948	-49.79999	0.00037	2190	100	767	
29	7.80473	-8.00397914	-8.00397914	-8.003979	0.000511	2077	100	2249	
30	6.365	-8.86310435	-8.86310435	-8.863104	0.000561	2433	100	1129	
Band	Gain1	Gain2	Vdc1	Vdc2		DNbb	DNSv	DNev	
31	-138.37		125	0.000317388	-0.014639		2280	100	2427
32	-186.78		125	0.000338213	-0.021057		2318	100	2459
33	-419.31		125	0.000285905	-0.039961		2566	100	1645
34	-490.88		125	0.000286037	-0.046804		2576	100	1444
35	-505.74		125	0.000284506	-0.047962		2588	100	1265
36	-482.76		125	0.000276546	-0.044502		2599	100	935
31hi	-78.581		125	0.000317388	-0.008314		1338	100	3172
32hi	-105.04		125	0.000338213	-0.011842		1347	100	3172

# Noise Equivalent Digital Number for Error Analysis

Band	NEdL	NEdDN
20	0.000957	1.74
21	0.015	0.65
22	0.0019	3.11
23	0.00217	3.10
24	0.00218	2.78
25	0.0062	7.46
27	0.0108	3.59
28	0.0172	4.96
29	0.00899	2.05
30	0.0219	5.63
31	0.00701	1.74
32	0.00606	1.64
33	0.0183	6.20
34	0.0161	5.65
35	0.0141	5.13
36	0.0154	5.82
31hi	0.247	34.92
32hi	0.198	30.11

NEdL

Table 3.3.4.2  
MODIS Thermal Bands

BAND	CENTER WAVELENGTH (nm)	TYPICAL SCENE TEMP Ttyp (K)	TYPICAL SPECTRAL RADIANCE Ltyp (*)	REQD NEdT (K)	NEdL (*)	MAX SCENE TEMP Tmax (K)	MAX SPECTRAL RADIANCE Lmax (*)	Lcloud
20	3750	300	0.45	0.05	0.000957	335	1.71	0.45
21	3959	335	2.38	2.00	0.015	500	86.00	0.67
22	3959	300	0.67	0.07	0.00190	328	1.89	0.67
23	4050	300	0.79	0.07	0.00217	328	2.16	0.79
24	4465	250	0.17	0.25	0.00218	264	0.34	1.44
25	4515	275	0.59	0.25	0.00620	285	0.88	1.53
26 (moved to Table 3.3.4.1)								
27	6715	240	1.16	0.25	0.0108	271	3.21	6.87
28	7325	250	2.18	0.25	0.0172	275	4.46	8.10
29	8550	300	9.58	0.05	0.00899	324	14.54	9.58
30	9730	250	3.69	0.25	0.0219	275	6.34	9.92
31	11030	300	9.55	0.05	0.00701	324	13.25	9.55
31hi	11030	400	29.1	1.00	0.247	400	29.08	9.55
32	12020	300	8.94	0.05	0.00606	324	12.10	8.94
32hi	12020	400	25.1	1.00	0.198	400	25.07	8.94
33	13335	260	4.52	0.25	0.0183	285	6.56	7.94
34	13635	250	3.76	0.25	0.0161	268	5.02	7.71
35	13935	240	3.11	0.25	0.0141	261	4.42	7.48
36	14235	220	2.08	0.35	0.0154	238	2.96	7.25

\* = Watts/m<sup>2</sup>/um/sr

Note: The high range of nonlinear bands 31 & 32 is 324K to 400K.

## Blackbody Estimated Emissivity due to Polarization Effects

Band	OBC Blackbody Emissivity
20	.9920
21	.9919
22	.9919
23	.9918
24	.9916
25	.9916
27	.9949
28	.9961
29	.9968
30	.9960
31	.9951
32	.9938
33	.9913
34	.9903
35	.9893
36	.9884

## OBC Blackbody Spectral Radiance Determination

$$L_{\lambda,bb} = \epsilon_{bb} B_{\lambda,bb} + \frac{1-\epsilon_{bb}}{\pi} (\Omega_{cav} B_{\lambda,cav} + \Omega_{ev} B_{\lambda,Earth})$$

where

<sup>effective</sup>  
<sub>solid angle</sub>

$\Omega_{cav}$  is the effective solid angle of the scan cavity subtended at the blackbody

$\Omega_{ev}$  is the effective solid angle of the Earth view porthole visible to the blackbody

$\epsilon_{bb}$  is the effective emissivity of the blackbody

12 thermistors averaged to obtain one effective temperature for the blackbody

Small gradient expected

Focal plane "footprint" covers about 90% of the blackbody for any single data sample

Thermistors which sufficiently deviate from the mean will not be used

Scan cavity temperature algorithm TBD

$L_{\lambda,bb}$  will be averaged

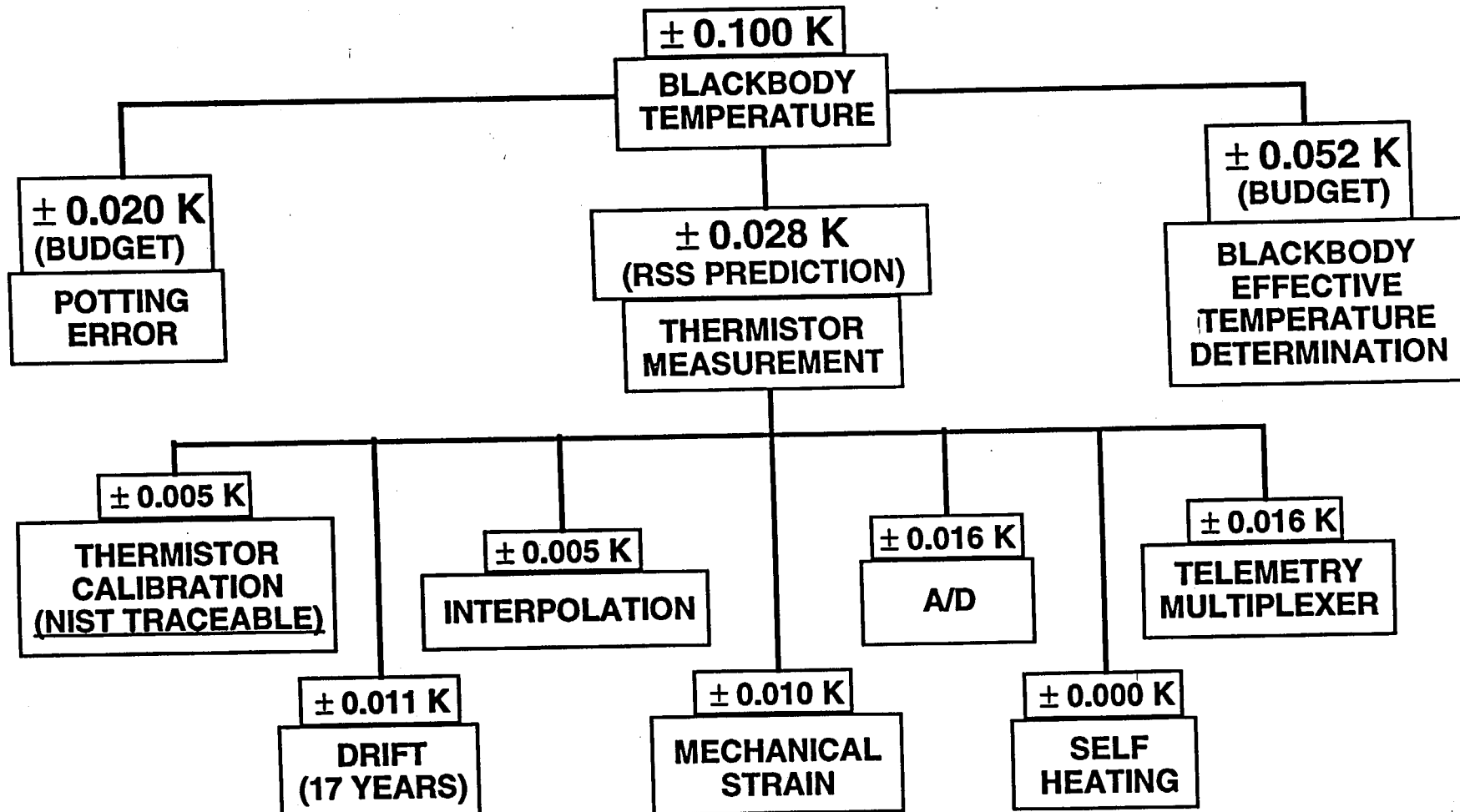
Effective Earth temperature algorithm TBD



# BLACKBODY TEMPERATURE ACCURACY MEETS $\pm 0.1$ K REQUIREMENT

**HUGHES**

SANTA BARBARA RESEARCH CENTER®  
a subsidiary



# Test Conditions for Determining Nonlinear Coefficient

Instrument Temperature			
Patch Temperature	Low	Nom	Hi
Low	✓	✓	
Nom	✓	✓	✓
Hi		✓	

Traditional vs non-traditional algorithm argument is based on this incomplete 3 X 3 grid

Historically a 4 X 4 grid has been used (AVHRR)

\*\* Check marks denote possible higher priority tests

# **Traditional Vs Non-Traditional Calibration Approach**

Argument is attributed to financially challenged test conditions

**Traditional** Calibrates in terms of difference between blackbody and space view signal.

Advantages      Tested and used on previous instruments

Disadvantages      Requires pre-launch testing at a multitude of instrument temperatures.

Can account for background drift only with instrument telemetry.

**Non-Traditional** Calibrates in terms of total detector radiant power.

Advantages      Accounts for background drift using both instrument and calibrator telemetry  
                    Does not require pre-launch testing at multiple instrument temperatures

Disadvantages      Not tested or used on other instruments

## **Similarities**

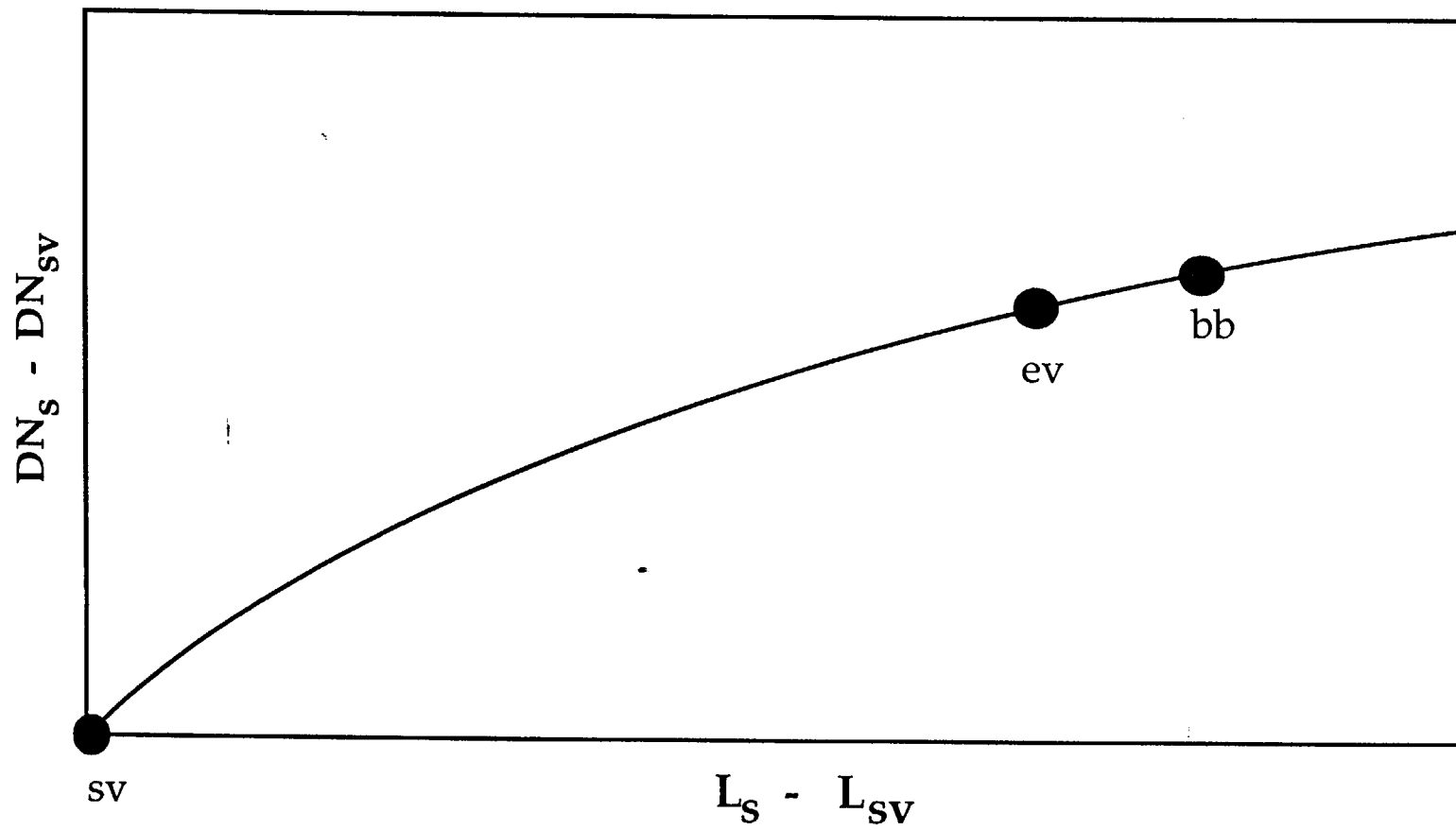
Master curve nonlinear term concept

Nonlinear term treated as a function of both patch and instrument temperature

Master curve 1st order gain term calibrated every scan

DC restore corrections necessary

## MODIS Calibration Curve (Traditional)



## Traditional Based Thermal Algorithm as Applicable to MODIS

Traditional form of thermal algorithm

$$DN_s = a(L_s)^2 + b(L_s) + DN_{sv}$$

Gain corrected form due to on-orbit setting of electronic gains

$$DN_s = \frac{Ga}{G_{pre}}(L_s)^2 + \frac{Gb}{G_{pre}}(L_s) + DN_{sv}$$

Mirror reflectivity scan angle dependence accountability form

$$DN_s = \frac{Ga}{G_{pre}}(L_s - L_{sv})^2 + \frac{Gb}{G_{pre}}(L_s - L_{sv}) + DN_{sv}$$

where

$$L_s = \sum_{\lambda=\lambda_1}^{\lambda_n} ((1 - \rho_{\lambda,s})B_{\lambda,mir} + \rho_{\lambda,s}L_{\lambda,s})R_{\lambda,opt}\Delta\lambda$$

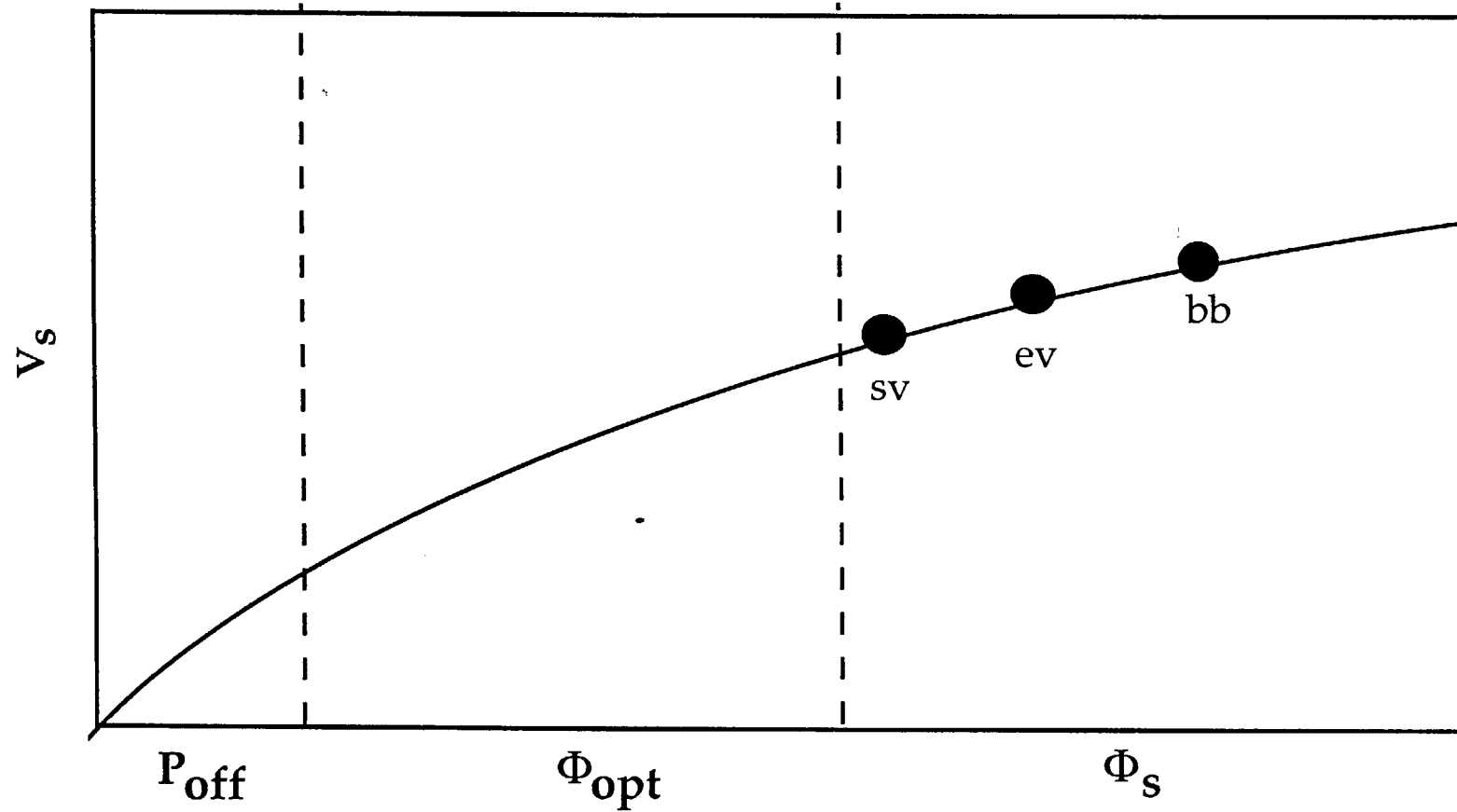
Nonlinear term on-orbit correctability form

$$\begin{aligned} \text{DN}_s = & \frac{G\alpha b^2}{G_{\text{pre}}} \left( \sum_{\lambda=\lambda_1}^{\lambda_n} ((\rho_{\lambda,sv} - \rho_{\lambda,s}) B_{\lambda,\text{mir}} + \rho_{\lambda,s} L_{\lambda,s}) R_{\lambda,\text{opt}} \Delta\lambda \right)^2 \\ & + \frac{Gb}{G_{\text{pre}}} \left( \sum_{\lambda=\lambda_1}^{\lambda_n} ((\rho_{\lambda,sv} - \rho_{\lambda,s}) B_{\lambda,\text{mir}} + \rho_{\lambda,s} L_{\lambda,s}) R_{\lambda,\text{opt}} \Delta\lambda \right) + \text{DN}_{sv} \end{aligned}$$

Spacecraft manuever scan mirror contamination form

$$\begin{aligned} \text{DN}_s = & \frac{G\alpha b^2}{G_{\text{pre}}} \left( \bar{\delta}_{s/bb} \sum_{\lambda=\lambda_1}^{\lambda_n} \rho_{\lambda,s} (L_{\lambda,s} - B_{\lambda,\text{mir}}) R_{\lambda,\text{opt}} \Delta\lambda + \bar{\delta}_{sv/bb} \sum_{\lambda=\lambda_1}^{\lambda_n} \rho_{\lambda,sv} B_{\lambda,\text{mir}} R_{\lambda,\text{opt}} \Delta\lambda \right)^2 \\ & + \frac{Gb}{G_{\text{pre}}} \left( \bar{\delta}_{s/bb} \sum_{\lambda=\lambda_1}^{\lambda_n} \rho_{\lambda,s} (L_{\lambda,s} - B_{\lambda,\text{mir}}) R_{\lambda,\text{opt}} \Delta\lambda + \bar{\delta}_{sv/bb} \sum_{\lambda=\lambda_1}^{\lambda_n} \rho_{\lambda,sv} B_{\lambda,\text{mir}} R_{\lambda,\text{opt}} \Delta\lambda \right) + \text{DN}_{sv} \end{aligned}$$

## MODIS Calibration Curve (Non Traditional)



## Non-Traditional MODIS Thermal Algorithm

$$V_s = a(\Phi_s + \Phi_{opt} + P_{off})^2 + b(\Phi_s + \Phi_{opt} + P_{off})$$

Detector incident radiant flux can be expressed as

$$\Phi_s = \frac{\pi A_d}{4(f_{eff}^*)_{port}^2} \int_{\lambda=0}^{\infty} L_{\lambda, lamb} \tau_{\lambda, opt} d\lambda$$

where

$\Phi_s$  is radiant flux attributed solely to the scan mirror and scene

$\Phi_{opt}$  is radiant flux attributed solely to the optical system

$P_{off}$  is extrapolated detector power at the zero flux condition

$A_d$  is the image area of the detector

$f_{eff}^*$  is the effective focal ratioExpressed in term of telemetered information

Non-traditional form of thermal algorithm

$$V_s = \alpha m^2 \left( L_o + \bar{\delta}_{s/bb} \sum_{\lambda=\lambda_1}^{\lambda_n} \rho_{\lambda,s} (L_{\lambda,s} - B_{\lambda,mir}) R_{\lambda,opt} \Delta\lambda \right)^2 + m \left( L_o + \bar{\delta}_{s/bb} \sum_{\lambda=\lambda_1}^{\lambda_n} \rho_{\lambda,s} (L_{\lambda,s} - B_{\lambda,mir}) R_{\lambda,opt} \Delta\lambda \right)$$

where

$$L_o = \frac{4(f_{eff}^\#)_{port}^2}{\pi A_d T_{opt} \bar{k}_{opt} \bar{\delta}_{bb}} (\Phi_{opt} + P_{off}) + \frac{1}{\bar{\delta}_{bb}} \sum_{\lambda=\lambda_1}^{\lambda_n} B_{\lambda,mir} R_{\lambda,opt} \Delta\lambda$$

$$m = \frac{b\pi A_d T_{opt} \bar{k}_{opt} \bar{\delta}_{bb}}{4(f_{eff}^\#)_{port}^2}$$

$$\alpha = \frac{a}{b^2}$$

## Applying to on-orbit telemetry

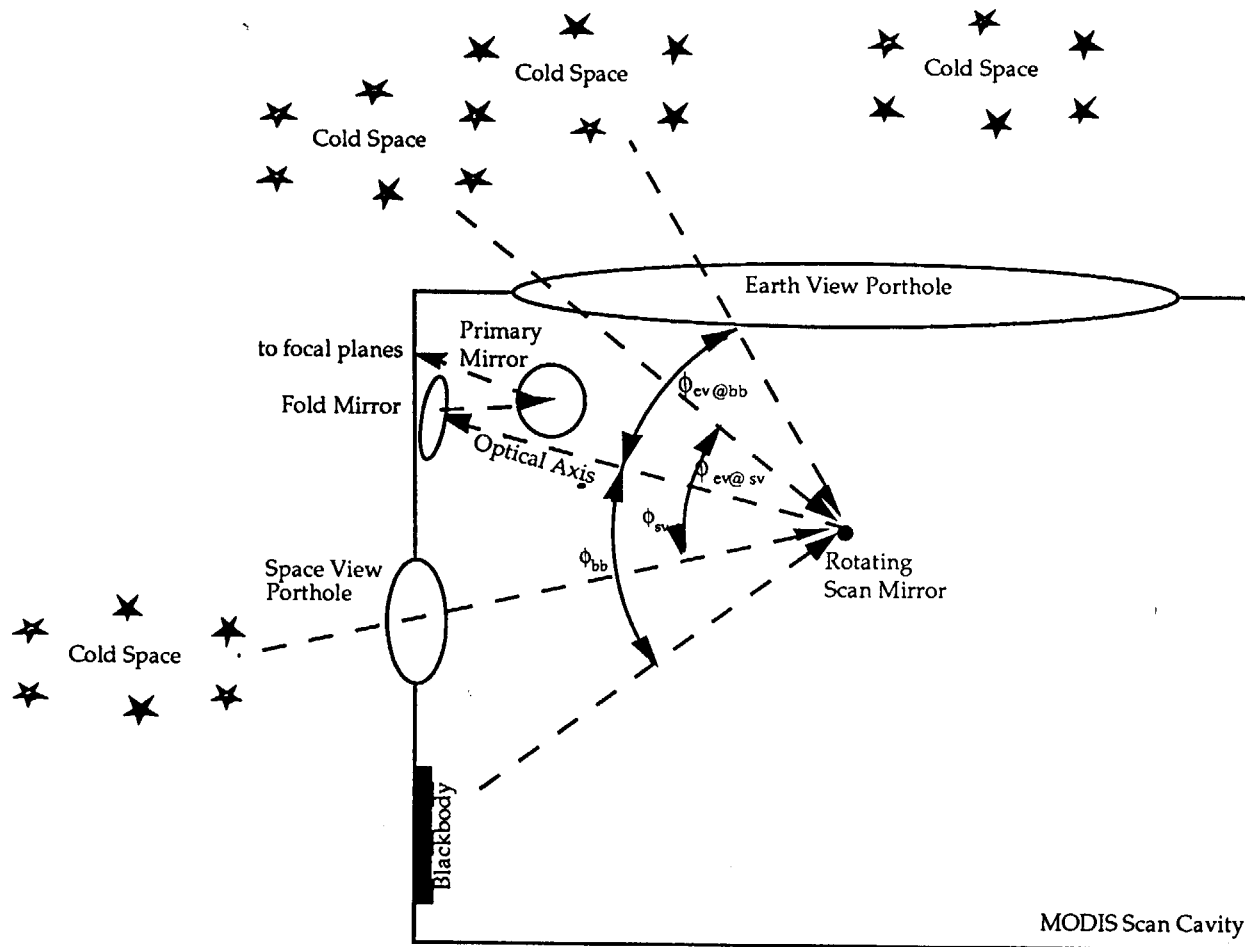
### PV Bands

$$\frac{\sum_{n=1}^N a_n (DN_s - DN_o)^n}{G_1 G_2 G_3 G_4} - V_{DC1} = \alpha m^2 \left( L_o + \bar{\delta}_{s/bb} \bar{L}_s \sum_{\lambda=\lambda_1}^{\lambda_n} \rho_{\lambda,s} R_{\lambda,opt} \Delta\lambda - \bar{\delta}_{s/bb} \sum_{\lambda=\lambda_1}^{\lambda_n} \rho_{\lambda,s} B_{\lambda,mir} R_{\lambda,opt} \Delta\lambda \right)^2 \\ + m \left( L_o + \bar{\delta}_{s/bb} \bar{L}_s \sum_{\lambda=\lambda_1}^{\lambda_n} \rho_{\lambda,s} R_{\lambda,opt} \Delta\lambda - \bar{\delta}_{s/bb} \sum_{\lambda=\lambda_1}^{\lambda_n} \rho_{\lambda,s} B_{\lambda,mir} R_{\lambda,opt} \Delta\lambda \right)$$

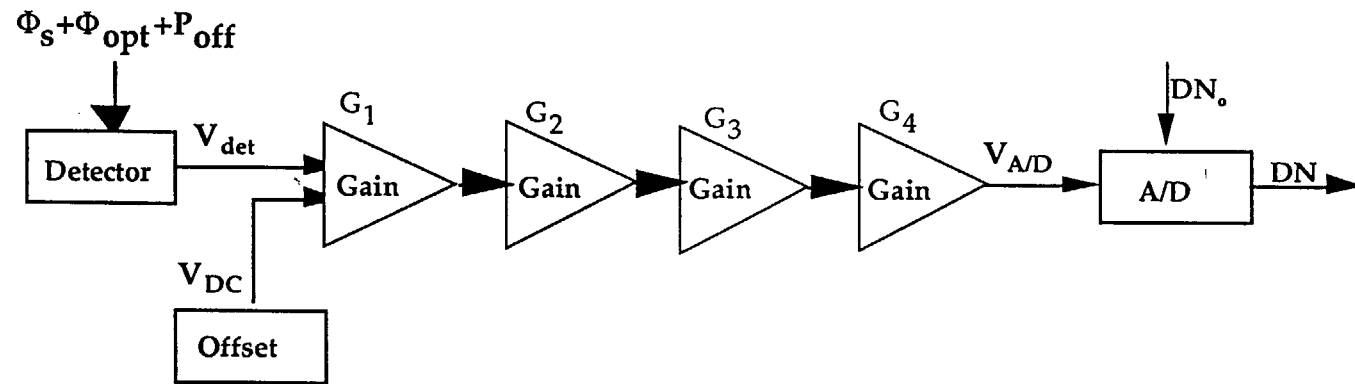
### PC Bands

$$\frac{\sum_{n=1}^N a_n (DN - DN_o)^n}{G_1 G_2} - \frac{V_{DC2}}{G_1} - V_{DC1} = \alpha m^2 \left( L_o + \bar{\delta}_{s/bb} \bar{L}_s \sum_{\lambda=\lambda_1}^{\lambda_n} \rho_{\lambda,s} R_{\lambda,opt} \Delta\lambda - \bar{\delta}_{s/bb} \sum_{\lambda=\lambda_1}^{\lambda_n} \rho_{\lambda,s} B_{\lambda,mir} R_{\lambda,opt} \Delta\lambda \right) \\ + m \left( L_o + \bar{\delta}_{s/bb} \bar{L}_s \sum_{\lambda=\lambda_1}^{\lambda_n} \rho_{\lambda,s} R_{\lambda,opt} \Delta\lambda - \bar{\delta}_{s/bb} \sum_{\lambda=\lambda_1}^{\lambda_n} \rho_{\lambda,s} B_{\lambda,mir} R_{\lambda,opt} \Delta\lambda \right)$$

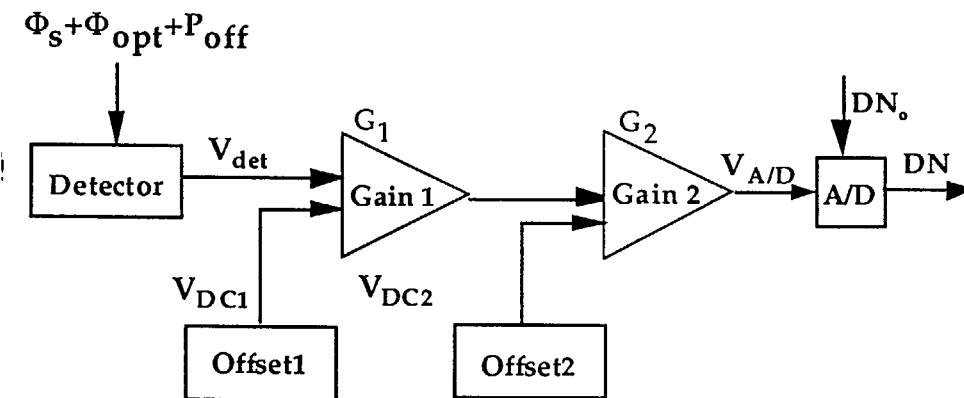
# Spacecraft Manuever for Scan Mirror Relative Angular Contamination Correction



## FPA Electronics



*Electronics circuit design for the photovoltaic bands*



*Electronics circuit design for the photoconductive bands*

# Three Point Source Pre-Launch Calibration

## Temporal Approach

Targets	On-board Blackbody Blackbody Calibration Source Space View Source *IAC (fire bands only)
Advantages	Minimal optical background differences between target data samplings
Disadvantages	Use of internal source

## External Source Approach

Targets	Blackbody Calibration Source Space View Source *IAC (fire bands only)
Advantages	All source external
Disadvantages	Optical background drift between target data samplings

\* This target may possibly be used for the less accurate fire bands since it can achieve a higher temperature

### Scan Mirror Polarization Factor

Wavelength um	26 deg PF Mirror	65 deg PF Mirror
3.75	0.00246522	0.01781625
3.959	0.00257608	0.01644125
4.05	0.00183071	0.01566043
4.465	0.0026929	0.01633859
4.515	0.00298998	0.01715603
6.715	0.00440368	0.01966586
7.325	0.00334134	0.02215427
8.55	0.01120478	0.10054851
9.73	0.01043451	0.09084717
11.03	0.00638524	0.05523017
12.02	0.00583872	0.05286712
13.335	0.01149319	0.09408547
13.635	0.01075171	0.10256485
13.935	0.01146021	0.10506176
14.235	0.01246831	0.11085346

### OBC Blackbody Polarization Factor

Wavelength μm	26 deg PF OBC Blackbody
4	0.0034
5	0.0032
6	0.0029
7	0.0023
8	0.0014
9	0.0025
10	0.0029
11	0.0031
12	0.0037
13	0.0042
14	0.0057

### Scan Mirror Polarization Factor

Wavelength um	26 deg PF Mirror	65 deg PF Mirror
3.75	0.00246522	0.01781625
3.959	0.00257608	0.01644125
4.05	0.00183071	0.01566043
4.465	0.0026929	0.01633859
4.515	0.00298998	0.01715603
6.715	0.00440368	0.01966586
7.325	0.00334134	0.02215427
8.55	0.01120478	0.10054851
9.73	0.01043451	0.09084717
11.03	0.00638524	0.05523017
12.02	0.00583872	0.05286712
13.335	0.01149319	0.09408547
13.635	0.01075171	0.10256485
13.935	0.01146021	0.10506176
14.235	0.01246831	0.11085346

### OBC Blackbody Polarization Factor

Wavelength μm	26 deg PF OBC Blackbody
4	0.0034
5	0.0032
6	0.0029
7	0.0023
8	0.0014
9	0.0025
10	0.0029
11	0.0031
12	0.0037
13	0.0042
14	0.0057